EUDET-Memo-2007-37

Status and Plans of the Large TPC Prototype for the ILC

T. Behnke[*], R. Diener[†], L. Hallermann[†*], P. Schade [†*]

May 20, 2008

Abstract

Within the EUDET programme, the FLC TPC Group at DESY in collaboration with the Department of Physics of the University of Hamburg is constructing a field cage for a large TPC prototype. This field cage is designed to fit into the PCMAG, a superconducting magnet which is installed at the electron test beam at DESY.
The setup –including various other parts like readout electronics, gas system, cosmic trigger and silicon hodoscope– will be available for development work towards a TPC for a detector at the International Linear Collider (ILC). Different groups from a worldwide collaboration will use this infrastructure to test their amplification and readout techniques.

[*]DESY, Hamburg, Germany
[†]University of Hamburg, Germany

1 Introduction

A Time Projection Chamber (TPC) is foreseen as the central tracking detector for at least two of the four detector concepts proposed for the future International Linear Collider (ILC). Within the EUDET programme, the FLC TPC Group at DESY in collaboration with the Department of Physics of the University of Hamburg is constructing a field cage for a Large Prototype (LP) of a Time Projection Chamber (TPC). The LP will have an inner diameter of 72 cm, which allows to test larger amplification and readout structures. With this diameter, the field cage can be used together with a silicon hodoscope inside a superconducting magnet (PCMAG), which is already installed in the electron test beam at DESY.

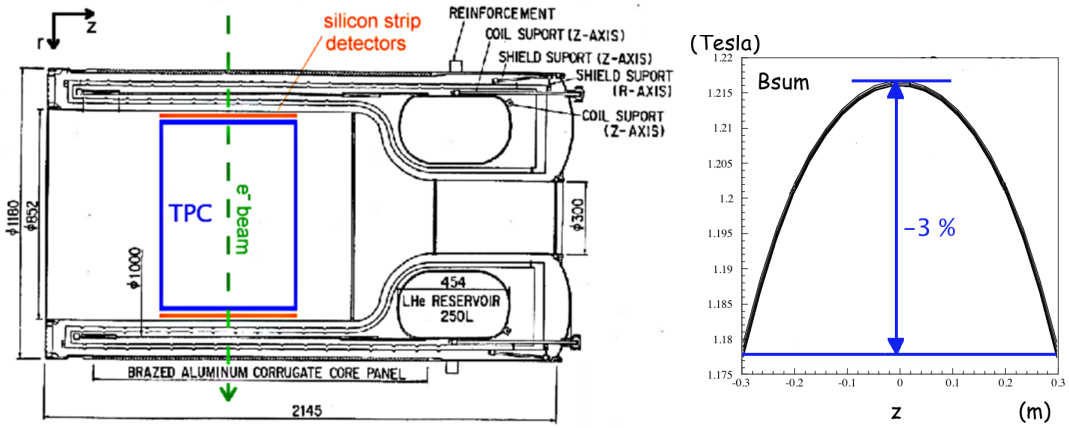

Figure 1: Technical drawing of the PCMAG (from [KEK]) and the result of a magnetic field calculation on the axis of the magnet (from [PCM]).

Figure 1 shows a technical drawing of the magnet and the result of a simple magnetic field calculation on the axis of the magnet. A detailed measurement and simulation of the magnetic field and its deviations is currently ongoing and is planned to be finished by the end of 2007.
The field cage is being constructed to be very lightweight but nevertheless stable and flexible to use. Therefore its structure will be made of composite materials which have already been used for the construction of smaller prototypes (see e.g. [Lux]). On the inside there will be a structure of field shaping bands (field strips), to provide a very homogeneous electric drift field. To ensure the needed high voltage stability, a special shielding layer is included between the field strips and the wall structure. The LP cage is foreseen to be available in 2008.

2 The Field Cage

2.1 Design of the Field Cage

The length of the field cage will be 61 cm. This is driven by the fact, that the magnetic field on the axis in the center of the magnet is homogeneous within 3 % only in a range of ±30 cm. As mentionend above, the inner diameter will be 72 cm and the outer diameter 77 cm. The current design is shown in Figure 2.

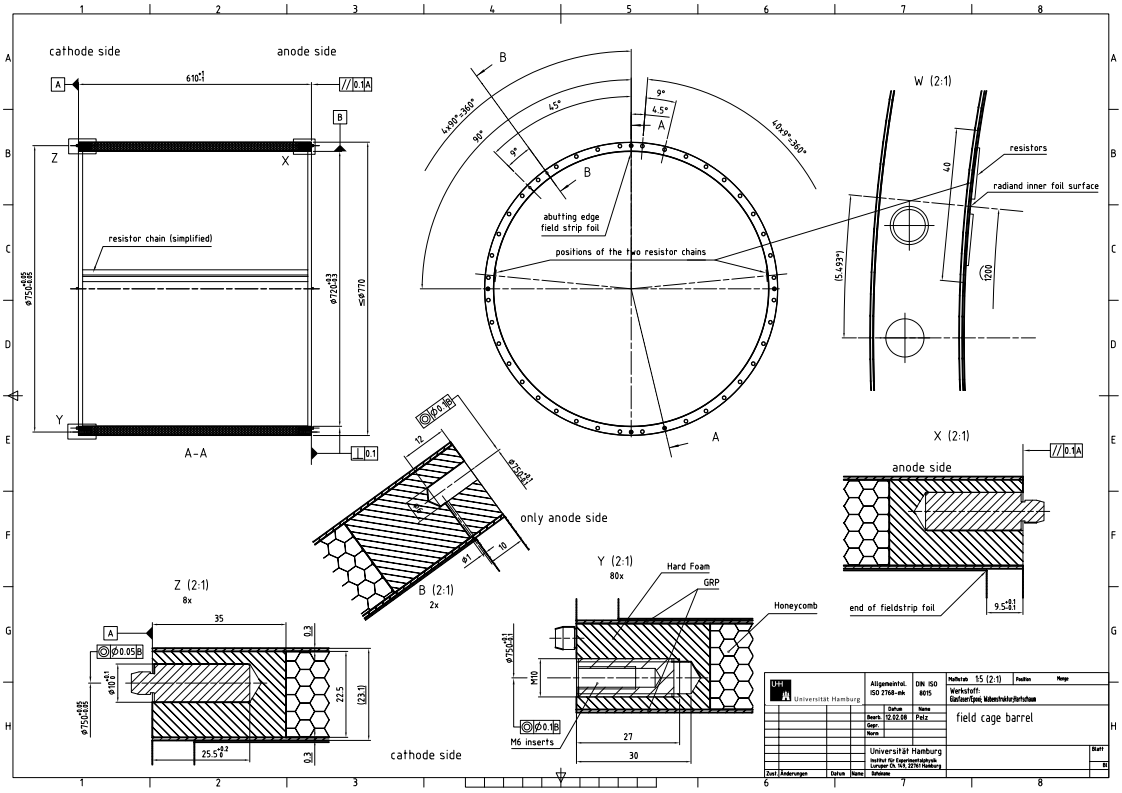

Figure 2: Technical drawing of the large prototype field cage.

2.2 Mechanical Calculations

With support from the ZM1 group (Central Design Group) at DESY, calculations of the mechanical stability of the composite structure of the field cage have been done. The goal of these calculations was to find a structure that is as thin as possible but nevertheless stable. Some results are shown in the Figures 3 and 4. For these calculations it has been assumed, that the two barrel ends are at a fixed position. This will be the case at the Large Prototype, since it will be attached to the end plates which are mounted on the support structure.

The left side of Figure 3 shows the bending of the field cage structure due to gravity. It is visible that the maximal deviation in the middle of the field cage is about 50 nm.

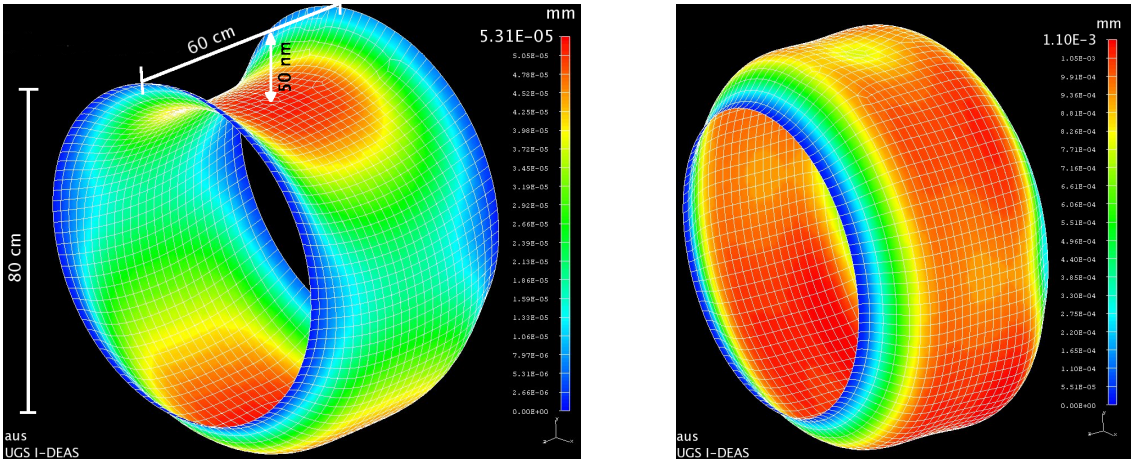

Figure 3: Calculation of the mechanical stability of the field cage showing the deviations from the perfect shape. Left side: under the force of gravity; right side: under the force of gravity and a slight overpressure.

If in addition a slight overpressure of a few millibars —which is about the amount of overpressure planned for the Large Prototype— is applied, the maximal deviation from the unloaded form is less than 1 μm (see right side of Figure 3). Figure 4 shows the stability of the structure under the pressure from a 5 kg point load placed in the middle of the cylinder. Here the deviation is about 400 nm.
The results show, that the proposed wall structure meets the demands. Structurally, the thickness of the GRP layers of the sandwich wall structure can be made very thin. The thickness has only a little influence on the mechanical stability of the wall. So the design of the wall profile was driven by the manufacturing. This lead to a design, in which to a 22.5 mm aramid honeycomb structure two 300 μm thick GRP layers are glued.

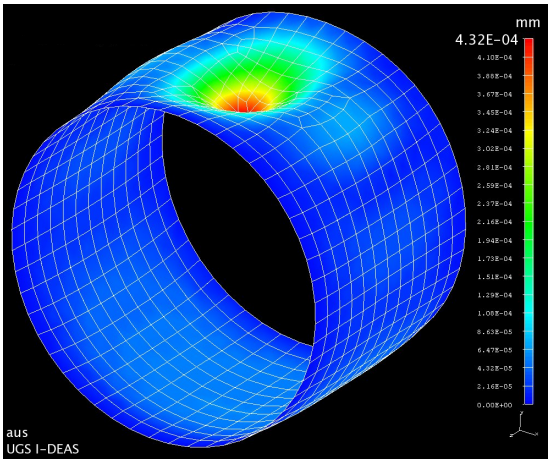

Figure 4: Calculation of the mechanical stability with a point load of 5 kg.

2.3 The Wall Structure

As mentioned above, the field cage wall should be very lightweight and stable. The light design is needed, since the TPC should introduce as little material as possible in front of the calorimeter in the final detector. This is needed to allow a high precision

energy measurement of the particles in the calorimetry by minimizing the energy loss in all detector parts inside the calorimeter. Therefore, the decision was made to use a composite structure which consists of two thin layers of Glass Reinforced Plastic (GRP) with a honeycomb structure made of aramid in-between. The GRP layers will each have a thickness of 300 μm and the honeycomb structure will have a thickness of 22.5 mm. On the outside there will be a 12.5 μm layer of Kapton which is coated on both sides by a thin layer of copper (5 μm). On the inside will be another 125 μm thick Kapton layer to electrically shield the field strip foil from the outside. The field strip foil will be the innermost layer. It is described in detail below. Figure 5 shows a schematic drawing of the profile of the field cage wall.

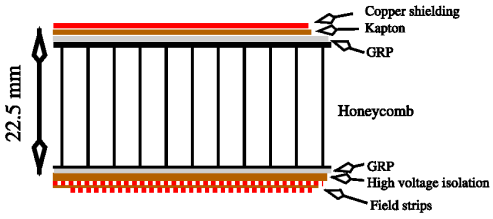

Figure 5: Schematic Drawing of the wall profile of the field cage wall of the Large TPC Prototype

The radiation length of this wall profile was estimated to be ca. 1.31 %. The radiation lengths and thicknesses of the different materials used to calculate this number are listed in Table 1. For this estimation, the copper layers of the field strip foil have been approximated by an continuous copper layer. The left side of Figure 6 shows an estimation of the fraction of the radiation length for the different materials of the wall structure in units of X_0. On the right side, the thicknesses of the different layers are shown in a sketch of the profile, including the epoxy layers that glue the other materials together.

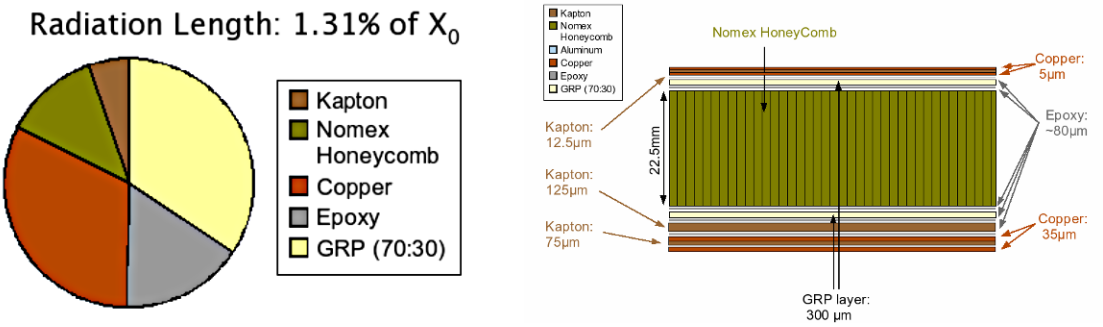

Figure 6: Estimation of the radiation length of the wall profile. Left side: fraction of the wall radiation length of the different materials; right side: wall profile.

2.4 Tests of the Wall Structure

The construction of the field cage will be done by an external company. To test the production procedure as well as the high voltage and mechanical stability of the wall structure, several sample pieces with different cross sections have been produced. These

Material	Radiation Length [cm]	Thickness	% of X_0
Kapton	28.57	$125 + 75 + 12.5\mu m = 0.02125cm$	0.07
Aramid Honeycomb	1430.00	$2.25cm$	0.16
Copper	1.43	$2 \times 5 + 2 \times 25\mu m = 0.006cm$	0.42
GRP (70:30)	13.31	$2 \times 300\mu m = 0.06cm$	0.45
Epoxy	19.40	$\sim 400\mu m = 0.04cm$	0.21

Table 1: Input values for the calculation of the radiation length of the field cage wall.

pieces differ in the high voltage shielding structures on the inside. A picture of one of these samples is shown in Figure 7.

The high voltage tests have been done with the setup shown in Figure 8. This setup consists of a acrylic glass cylinder which is gas tight to allow tests under different gas atmospheres. Inside this cylinder is a sample piece holder (also made of acrylic glass) with an electrode in the middle. The sample piece is placed on this holding structure. A second electrode is placed on top of the sample piece and then a high voltage up to 30 kV can be applied. To increase the area of the upper electrode, a small metal plane has been used between the electrode and the sample piece to exclude a systematic error due to a misalignment.

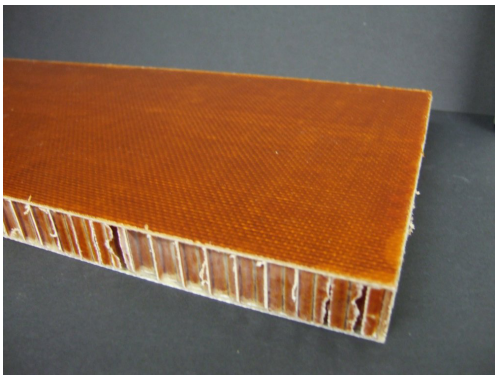

Figure 7: Sample piece of the field cage wall.

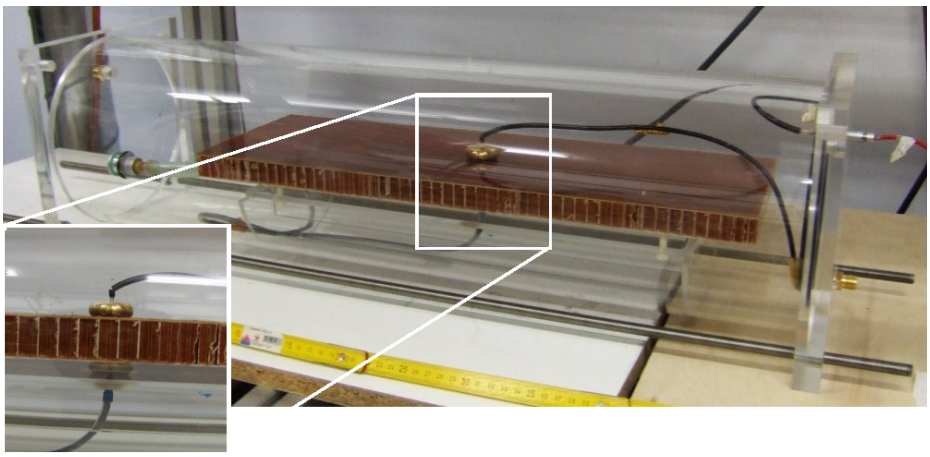

Figure 8: Setup for test of the high voltage stability of the field cage wall sample pieces.

The tests were done for all sample pieces for potentials of up to 24 kV. All pieces passed the test which lasted at least 24h each. After a modification of the setup, voltages up to 30 kV could be applied. With this setting only the sample piece with the least shielding

(only one layer of Kapton) has been tested. This sample piece is the preferred solution, since it is easiest to produce and its profile has the lowest material budget. This 24 hour test with a higher field has also been successful and no breakdown occurred.
To test the mechanical stability, a four point bending test has been performed with some of the samples (see Figure 9). These test have been done with the help of the Institute of Polymers and Composites of the Hamburg University of Technology (TUHH). The results of these tests show, that the chosen structure has sufficient strength.

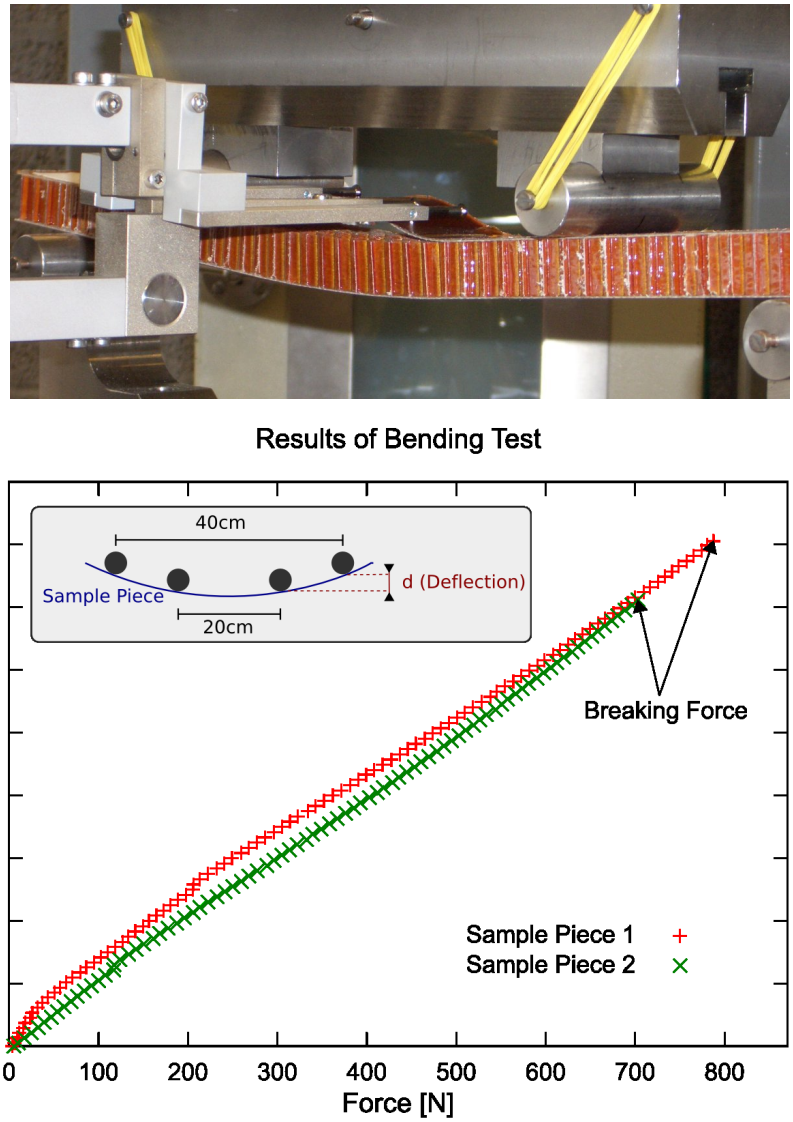

Figure 9: Top: Wall sample piece during the four point bending test at the Institute of Polymers and Composites of the TUHH.
Bottom: Test results for two sample pieces. The deflection d is plotted against the applied force F. A sketch of the setup is shown in the gray box.

2.5 The Field Strip Foil

As mentioned in the introduction, the field strip foil ensures homogeneously decreasing potentials from the cathode, which lies at a potential of more than 20 kV, down to the anode, which lies at ground potential.
These field strips are parallel rings that lie on potentials that are incrementally falling from the anode towards the cathode (Figure 10, for reference see for example [Lux] or [AHB]). The potentials on the field strips are set by a resistor chain, which connect the adjoining strips and the first and last strip to the cathode respectively the anode.
The field strips have a pitch of 2.8 mm and a width of 2.3 mm. The 0.5 mm gap between the strips has to be "closed" to avoid large field distortions. Otherwise, the lower potential of the external shielding is "visible" to the drifting electrons. This effect is called "*punch through*" and is illustrated in Figure 11. Here, the result of a field calculation is shown illustrating the equipotential lines in the vicinity of the chamber's wall.

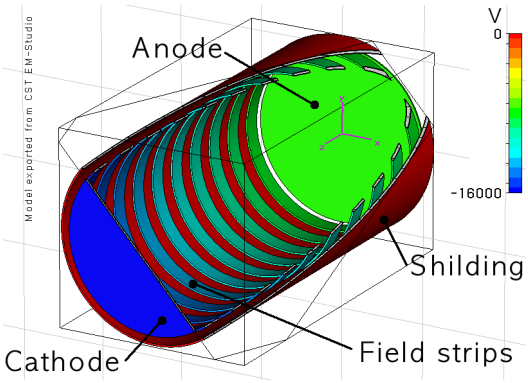

Figure 10: Schematic design of a cylindrical TPC

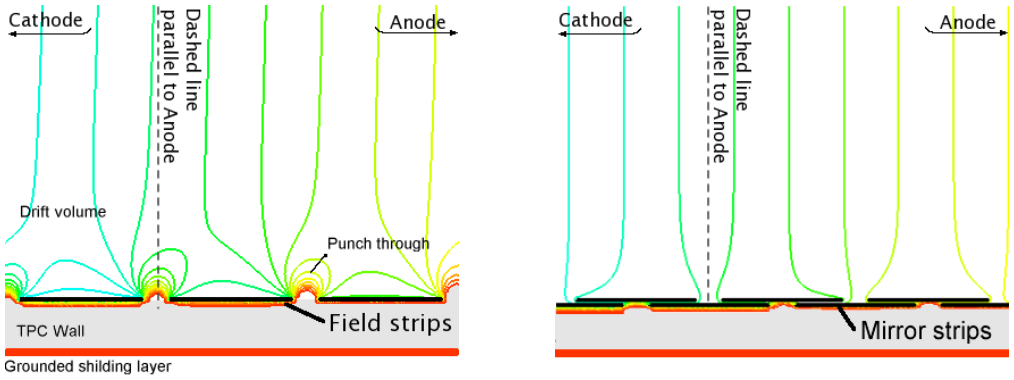

Figure 11: Equipotential lines of the the electric field with and without shielding mirror strips. Left side: punch through at the unshielded design; right side: field lines with shielding by mirror strips.

As the electric field vectors are perpendicular to the equipotential lines, these should be parallel to the anode (dashed line in figure 11). But due to the higher potential of the external shielding reaching through the gaps between the field strips, the equipotential lines get bend in direction of the cathode which causes radial drift field components and thus an imperfect field.

Due to fabrication and electrostatic operation issues[1] the gaps cannot be made narrower than 0.5 mm. Therefore, to avoid these distortions, mirror strips are located on the back of the foil. These mirror strips have the same dimensions as the field strips, but are displaced by half a pitch in respect to the field strips. Each mirror strip lies on an intermediate potential between the two adjoining field strips.

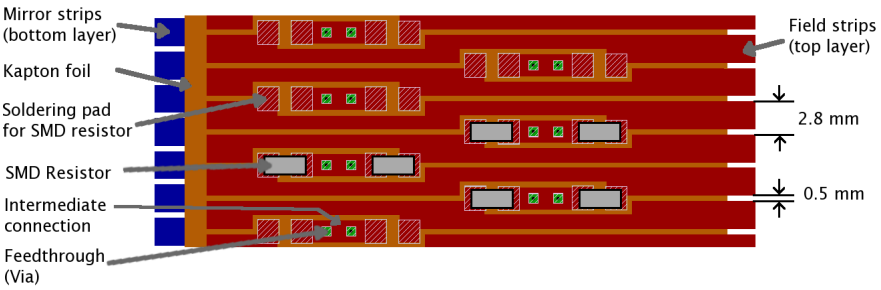

Figure 12: Sketch of the Layout of the field strip foil.

The potential is applied by vias from little "islands" which provide an intermediate connection. They are located between two strips and connected on each side to the field strips by a resistor. The chosen design is shown in Figure 12. The field strips are shown in red. Some extended mirror strips are shown in blue on the left side. The small hatched boxes on the "island" and the field strips are the connection points for the resistors (which are not shown in this sketch). The small green boxes on the intermediate connection depict the vias to the mirror strips. The resistors are shown as gray rectangles.
The field strip foil has been produced by a specialized company. Figure 13 shows the assembled foil. It is produced out of two foils which are glued together. The foils arrived at DESY in January. After gluing them together, they have been equipped with the resistors. After testing they will be shipped to the company building the field cage.

3 Field Calculations and Simulations

3.1 Field Calculations

To examine if the chosen construction plans for the field cage and the layout of the field strip foil ensure a homogeneous electric field, field calculations have been performed. These calculations have been done with a program that uses a finite element technique. In these calculations distortions due to manufacturing accuracies and resistors with a resistivity accuracy of $\pm 0.02\,\%$ have been taken into account. Figure 14 shows the distribution of the resitor values around the nominal value of $1\,\mathrm{M\Omega}$. This distribution has been derived from a measurement of a batch of real resitors and then it has been used in the calculation.

[1] The potential difference between two neighboring field strips can have a magnitude of up to 100 V.

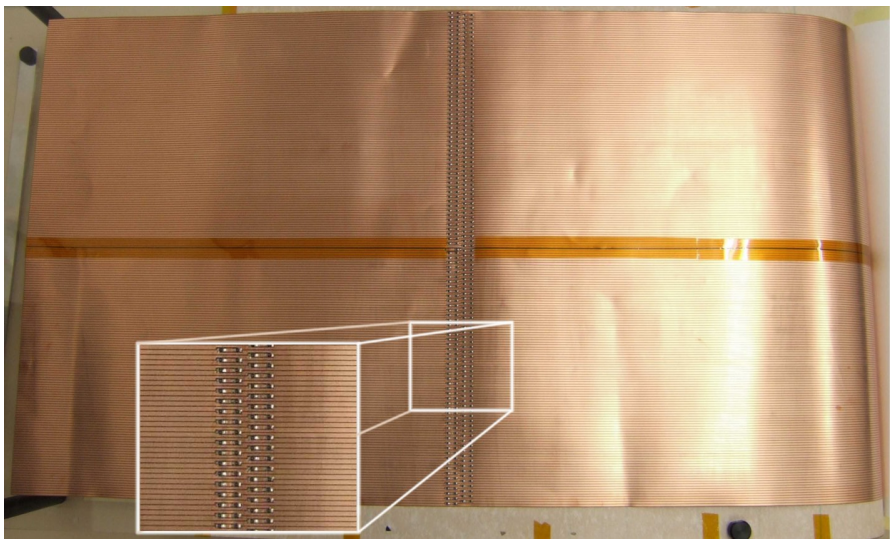

Figure 13: The assembled field strip foil with a zoom of a part of the resistor chain.

The field cage sides, to which the end plates will be mounted, can be produced with a precision of the parallelism of 100 μm. The slight tilt of the cathode respectively the anode due to this inaccuracy has been taken into account.
The field deviations are expressed in units of $\Delta E/E_{nominal}$, where $E_{nominal}$ is the expected field value at a certain point for a perfectly homogeneous field. ΔE is defined as $|E_{calculated} - E_{nominal}|$. Here, $E_{calculated}$ is the field value that results at this point from the calculation taken the limited accuracies into account. The goal is to ensure field deviations below $\Delta E/E_{nominal} \sim 10^{-4}$ (mean over whole chamber).

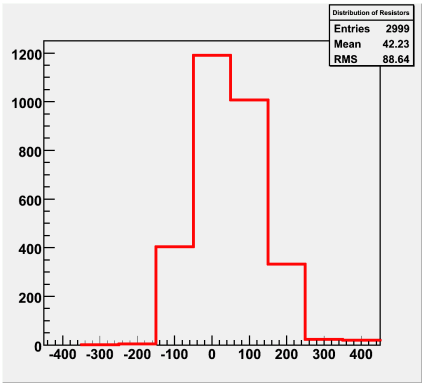

Figure 14: Distribution of the measured resistivity around the nominal value of 1 MΩ.

Figure 15 to 17 show the deviations ΔE from the perfect electrical field. A cut through the chamber along its symmetry axis is plotted. The anode is on the left side and the cathode on the right side of the plot. The color scale is chosen so that values of $\Delta E/E$ that are smaller than the deviation goal are plotted in shades of green. Values that are above the limit are plotted in red.
With a "*perfect*" setup there are basically no deviations from the perfect electric field, except for the area very close to the field cage walls. Close to the walls there are small deviations, which are well within limits (see Figure 15(a)). When the non-perfect resistors and an estimated finite resistivity of the wall are taken into account, the deviations are visible though nearly the whole chamber, but they are still within the limits (see Figure 15(b)).
If in addition a tilt of 200 μm of the cathode is taken into account, the deviations grow

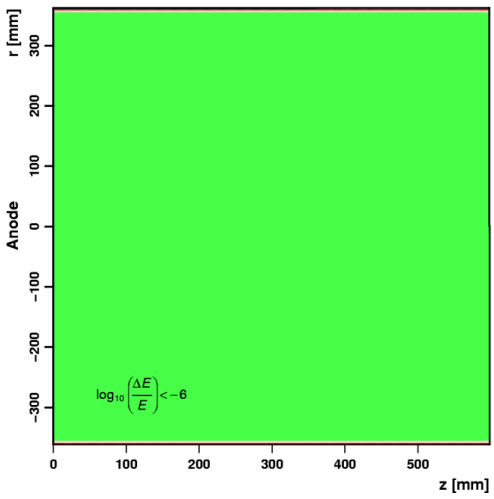

(a) Field deviations for a perfect setup with 2.3 mm field and mirror strips and 0.5 mm gaps.

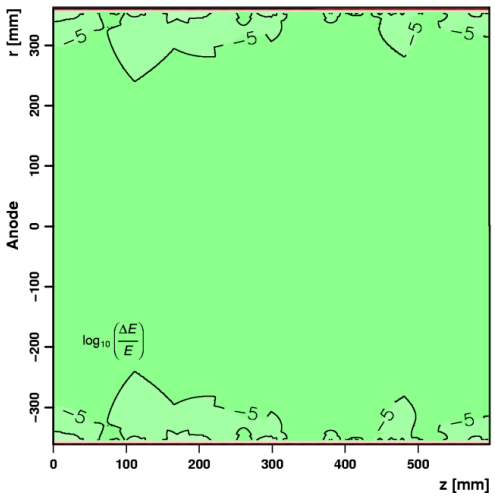

(b) 'Field deviations for a realistic resistor distribution (see Figure 14) and finite resistivity of the wall.'

Figure 15: Electric field deviations from the perfect field in units of $\Delta E/E_{nominal}$.

larger (see Figure 16). Near the cathode, they even grow larger than the deviation limit of 10^{-4}. Since these large deviations are limited to the area near the cathode, they influence only the drift of electrons in this region. Due to the limited length that the electrons drift in this distorted field, the effect of these deviations is not critical.

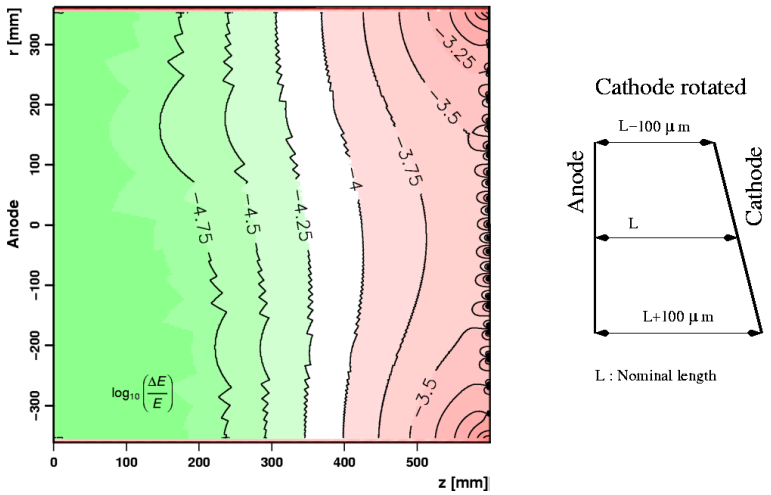

Figure 16: Electric field deviations in units of $\Delta E/E_{nominal}$ when a realistic resistor distribution and a tilted cathode (by 200 μm) is taken into account (see sketch on the right side).

Figure 17 shows the deviations when in addition to the cathode also the anode is tilted by 200 μm. Here, the effect of the two tilted end plates level out to a certain extent and the field is almost symmetric. In average the field deviations are tolerable, but in the corners of the drift volume they rise well above the deviation limit.

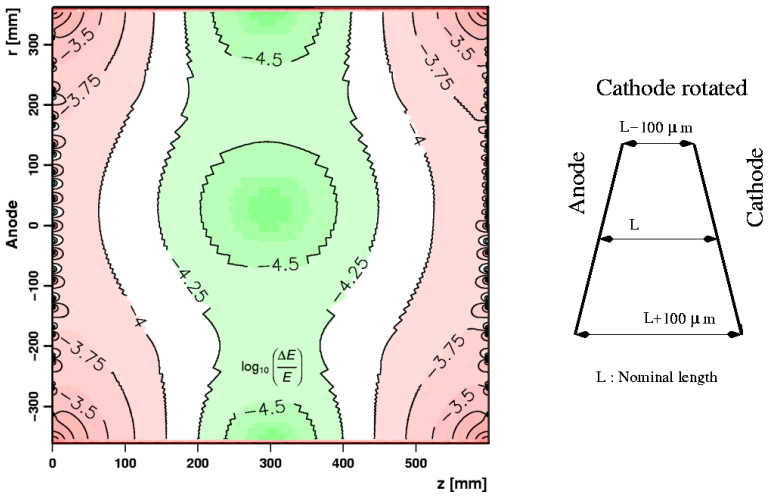

Figure 17: Electric field deviations in units of $\Delta E/E_{nominal}$ when a realistic resistor distribution and a tilted cathode and anode (each by 200 μm) is taken into account (see sketch on the right side).

To judge the effect of the field deviations, the displacement of an electron that drifts in these fields from the drift path that the electron would follow in a perfect field has been simulated. This simulation works on a 200×200 μm grid and calculates the displacement of the electron on each step on this grid over the whole drift path.
As shown in Figure 18, the calculation of the maximal displacement $|\Delta r|$ for a measured arrival coordinate at the anode is calculated. This is done by using an iterative method. Starting from the anode, the drift path of the electron is computed in steps. This corresponds to following a positron in the same field in the opposite direction.
Taking the field strengths into account, a drift time can be determined for each starting position of the electron — corresponding to each end position of the positron. The longitudinal displacement Δz can then be calculated by the difference between the expected z position for a perfect field and the nominal drift velocity and the real z position at a certain point. The maximum of all these displacements, denoted by Δz, is shown in the following evaluation.
Figure 19 shows the results of the calculations. Here, the displacements are plotted against the radius r, where the electron is measured on the anode. It is visible, that in the center of the chamber, the total displacement is below 10 μm, the longitudinal displacement is even an order of magnitude smaller. Near the field cage walls at a radius of 300 mm or higher, the total displacement grows up to 100 μm. This value is about the resolution that should be achieved. Therefore, these displacements will have to be corrected in the reconstruction software.

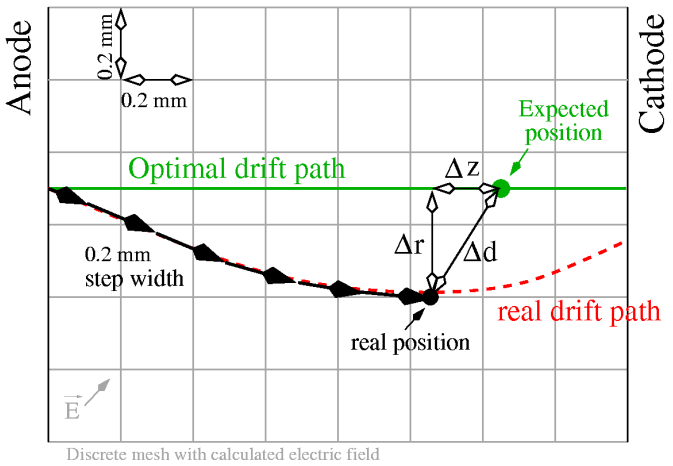

Figure 18: Reverse drift to calculate the radial and the longitudinal displacements of the drifting electrons in an inhomogeneous electric field. In the evaluation, the maximal displacement $|\Delta r|$ and Δz is shown.

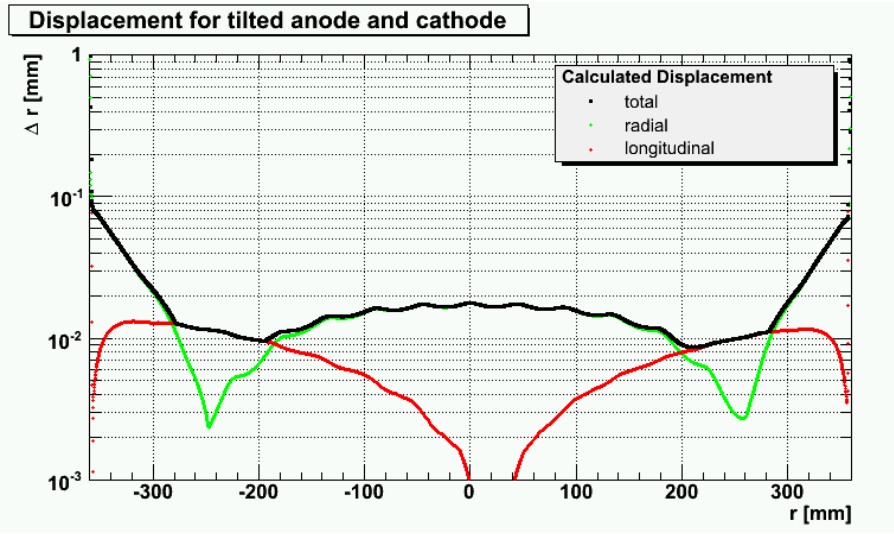

Figure 19: Maximal displacement of the measured electron at the anode for a calculation with a tilted anode and cathode as well as imperfect resistors (see text and Figure 17). The radial displacement Δr, the longitudinal displacement Δz and the resulting total displacement is shown.

Further efforts are ongoing in this area. For example, the field deviations due to the gap between the anode respectively the cathode end plates and the field strips will be considered. In the next step, the magnetic field and its inhomogeneities will be considered. While it is expected that a perfect magnetic field would reduce the displacements, since the electrons tend to follow rather the magnetic than the electric field lines, an inhomogeneous magnetic field can lead to much larger displacements.

The results of these calculations will serve as an important input for the reconstruction software. If they are well known, they can be incorporated in the reconstruction process and the errors can be corrected. Therefore, besides the calculation of the effects, also means to measure and calibrate the chamber are under consideration. These include evaluating the information of the silicon hodoscope as well as a laser system which produces well known tracks.

4 Summary

The construction plans for the field cage for the large TPC prototype have been finalized. This includes the wall structure as well as the field strip foil. The construction itself will be done by external companies, which have been included in the discussion of the design process. Also, other groups of the EUDET framework and groups worldwide that are active in TPC research and development have been included in this discussion. The field cage will be ready at the test beam area at DESY when the experimental groups arrive in 2008.
The simulation of the properties of the field cage design and the tests of sample pieces show good results. The mechanical and electrical stability of the design should be more than sufficient. The homogeneity of the electric field is not perfect, but this effect will be corrected in the reconstruction software. There, a correction of field inhomogeneities is also needed due to the field deviations of the 1 T magnet PCMAG, which is already installed at the DESY test beam area. The radiation length of the wall structure is still above the goals, but with slight modifications, it should be feasible to reach the goal of a radiation length of below 1 % of X/X_0.

Acknowledgment

This work is supported by the Commission of the European Communities under the 6^{th} Framework Programme “Structuring the European Research Area” contract number RII3-026126.

References

[KEK] A. Yamamoto, *Proceedings of the 5th Workshop on Balloon Borne Experiment With A Superconducting Magnetspectrometer*, KEK Proceedings 94-11, KEK 1995

[PCM] Sakamoto, Sugiyama, *B calculations of S-JACEE magnet*, Saga univ.

[Lux] T. Lux, *Studies for a time projection chamber for the International Linear Collider and measurement of beauty cross sections in deep inelastic scattering at HERA*, DESY-THESIS-2005-019-2005-019, DESY 2005

[EUP] T. Behnke, L. Hallermann, P. Schade, R. Diener, *The field cage for a large TPC prototype*, EUDET-Memo-2006-03, EUDET 2006

[AHB] C. Bowdery, 1995 Aleph Handbook, Vol.1, European Organisation for nuclear Research - CERN, Geneva 1995